

# A New Apolipoprotein B Truncation (apo B-43.7) in Familial Hypobetalipoproteinemia: Genetic and Metabolic Studies

Neelam Srivastava, Davide Noto, Maurizio Averna, Judit Pulai, Rai Ajit K. Srivastava, Thomas G. Cole, Mickey A. Latour, Bruce W. Patterson, and Gustav Schonfeld

We describe a new truncation of apolipoprotein (apo) B in a white kindred with familial hypobetalipoproteinemia (FHBL). Apo B-43.7, found in a daughter and her father, was due to a C → T change in base position 6162 of the apo B gene converting the arginine (residue 1986) codon CGA to a stop codon TGA. Both subjects were heterozygotes, and both apo B-43.7- and apo B-100-containing particles were present in plasma. On density gradient ultracentrifugation (DGUC), approximately 30% to 40% of apo B-43.7 floated with very-low-density lipoprotein (VLDL)/intermediate-density lipoprotein (IDL)-density particles and 60% to 70% floated with high-density lipoprotein (HDL)-density particles. To assess the metabolism of apo B, <sup>13</sup>C-leucine was infused and its rates of appearance in and disappearance from apo B-43.7- and apo B-100-containing particles were quantified by multicompartmental kinetic analysis. Apo B-100 entered plasma via VLDL with a production rate of 30 mg · kg<sup>-1</sup> · d<sup>-1</sup>. Fractional catabolic rates (FCRs) for apo B-100 VLDL, IDL, and low-density lipoprotein (LDL) were 20.0, 16.0, and 0.46 pools · d<sup>-1</sup>, respectively. The production rate of apo B-43.7 was 9.6 mg · kg<sup>-1</sup> · d<sup>-1</sup>, and FCRs for apo B-43.7 VLDL- and HDL-like particles were 12.0 and 1.8 pools · d<sup>-1</sup>, respectively. Approximately 30% of apo B-43.7 in HDL-density particles was derived from VLDL apo B-43.7, and about 70% appeared to enter the plasma as HDLs. The relatively low production rate of apo B-43.7 is compatible with previous reports that apo B truncations are produced at lower rates than their apo B-100 counterparts.

Copyright © 1996 by W.B. Saunders Company

FAMILIAL hypobetalipoproteinemia (FHBL) is an autosomal codominant condition characterized by abnormally low levels of apolipoprotein (apo) B and low-density lipoproteins (LDLs).<sup>1</sup> Apo B circulates in plasma in two forms, apo B-100 and apo B-48. In humans, apo B-100 is synthesized by the liver and found in very-low-density lipoproteins (VLDLs), intermediate-density lipoproteins (IDLs), and LDLs, whereas apo B-48 is synthesized almost exclusively by the intestine and is a structural component of chylomicrons and chylomicron remnants.<sup>2</sup> Apo B-48 results from the posttranscriptional editing of intestinal apo B-100 mRNA. Nucleotide C at position 6666 in the apo B gene is deaminated to a U, changing a *glu* codon, CAA, to the stop codon, UAA.<sup>3</sup> High plasma concentrations of apo B and LDL predispose individuals to premature atherosclerosis,<sup>4</sup> whereas low plasma levels of apo B and LDL are likely to be beneficial in terms of coronary heart disease risk.

In many FHBL kindreds, the low plasma LDL phenotype is not associated with any detectable size abnormalities of apo B in plasma. However, in some kindreds, the FHBL phenotype cosegregates with any of several truncated species of apo B detectable in plasma ranging in size from apo B-27.6 to apo B-89.<sup>1,5-12</sup> In a few kindreds, truncation-producing mutations are present that specify the translation of proteins shorter than apo B-27.6. These short proteins are not detectable in plasma.<sup>1</sup> Finally, there are

kindreds in which the FHBL phenotype is not linked to the apo B gene.<sup>13</sup>

Truncated forms of apo B may result from a variety of frame-shifting or nonsense mutations that produce premature translational stop codons.<sup>1,5</sup> Putative homozygotes or compound heterozygotes in some FHBL kindreds have only trace amounts of apo B in the plasma and may show symptoms of fat malabsorption and fat-soluble vitamin deficiency.<sup>14</sup> Heterozygotes, on the other hand, are usually asymptomatic even though their plasma apo B and LDL cholesterol levels are well below the fifth percentile. The plasma of subjects heterozygous for apo B truncations usually contains distinct apo B-100- and apo B truncation-containing lipoprotein particles that manifest differences in size and metabolism.<sup>5-12</sup>

We report a newly identified FHBL kindred with a new species of truncated apo B, apo B-43.7. This report describes the gene mutation responsible for apo B-43.7 and the distribution of the truncation among major classes of lipoproteins. Additionally reported is the metabolism of apo B-100 and apo B-43.7 in one of the heterozygotes.

## SUBJECTS AND METHODS

### Subjects

The members of the M kindred are described in Table 1 and Fig 1. The proband was asymptomatic and taking no medication. The study protocol was approved by the Human Studies Committee of Washington University School of Medicine. Blood was drawn from fasted individuals into tubes containing EDTA (1 mg/mL). The samples were then divided into aliquots and stored at -70°C for isolation of genomic DNA. Plasma samples, obtained by centrifugation, were stored at -70°C for immunoblotting.

### Plasma Lipids and Lipoproteins

Total cholesterol (TC), triglycerides, and LDL and high-density lipoprotein (HDL) cholesterol were determined by the Lipid Research Center Core Laboratory at Washington University School of Medicine using commercially available kits (Technicon Instruments, Tarrytown, NY). Lipoprotein fractions were isolated by

From the Division of Atherosclerosis, Nutrition and Lipid Research, Department of Internal Medicine, Washington University School of Medicine, St Louis, MO.

Submitted February 8, 1996; accepted May 7, 1996.

Supported in part by National Institutes of Health Grant No. HL0142460, General Clinical Research Center Grant No. USPHS MO1RR00036, and Diabetes Research Training Center Grant No. NIH5P60DK20579.

Address reprint requests to Gustav Schonfeld, MD, MO 63110.

Copyright © 1996 by W.B. Saunders Company

0026-0495/96/4510-0018\$03.00/0

**Table 1. Characteristics of the Affected and Unaffected Members of the Apo B-43.7 Kindred**

Pedigree Position	Sex	Date of Birth	Weight (kg)	Height (cm)	TC (mg/dL)	TG (mg/dL)	LDL-C (mg/dL)	HDL-C (mg/dL)	Apo B (mg/dL)	Apo AI (mg/dL)	Apo E Genotype
I-1*	M	7/35	100	183	174 (<25)	94 (<50)	95 (<10)	59 (<90)	63 (<10)	172	E <sub>3</sub> /E <sub>3</sub>
I-2	F	1/38	81	173	186 (<25)	105 (<50)	100 (<25)	62 (50)	87 (<50)	196	E <sub>3</sub> /E <sub>3</sub>
II-1*	F	6/61	55	170	111 (<5)	32 (<5)	47 (<5)	55 (50)	40 (<5)	183	E <sub>3</sub> /E <sub>3</sub>
II-2	M	9/58	77	178	166 (<25)	77 (<25)	88 (<10)	61 (<95)	66 (<50)	160	E <sub>3</sub> /E <sub>3</sub>
II-3	F	8/64	73	175	189 (<75)	70 (<50)	103 (<50)	71 (<90)	84 (>50)	183	E <sub>3</sub> /E <sub>3</sub>
III-1	M	8/87	27	133	142 (<25)	39 (<25)	88 (<50)	44 (<25)	66 (>50)	116	E <sub>3</sub> /E <sub>3</sub>

NOTE. Numbers in parentheses are age-, sex-, and race-matched percentiles (lipids<sup>34</sup> and apo B<sup>36</sup>).

Abbreviation: TG, triglycerides.

\*Affected.

established protocols of the Lipid Research Clinics.<sup>15</sup> Plasma apo AI and apo B were determined by immunonephelometry (Behring, Somerville, NJ). Freshly drawn plasma samples (1.5 mL) were subjected to gel permeation chromatography on a fast protein liquid chromatography (FPLC) system (Pharmacia, Uppsala, Sweden)<sup>7,11,12</sup> and also to density gradient ultracentrifugation ([DGUC] 14 mL).<sup>7</sup> The resultant fractions were analyzed for TC and also for apo B-100 and apo B-43.7 as previously described.<sup>7,11,12,16</sup>

#### Sodium Dodecyl Sulfate-Polyacrylamide Gel Electrophoresis Analysis and Immunoblotting

Apo B species were immunoprecipitated from plasma,<sup>11</sup> and the immunoprecipitates were electrophoresed as described previously.<sup>9,11,17</sup> After electrophoresis, the proteins were electrotransferred to Immobilon-P membranes (Millipore, Bedford, MA) and probed with an anti-apo B monoclonal antibody (C1.4).<sup>18</sup> Enhanced chemiluminescence and Western blotting detection reagents (Amersham International, Amersham, UK) were used according to the manufacturer's recommendation.

#### DNA Preparation

Genomic DNA was prepared from whole blood by a commercially available kit (Puregene; Gentrasystem, Minneapolis, MN).

#### Single-Stranded Conformational Polymorphism

Single-stranded conformational polymorphism (SSCP) was performed according to the method of Orita et al<sup>19,20</sup> with some

modifications. Several sets of primers in the apo B gene region spanning nucleotides 5840 to 6653 were used to obtain 200 to 300-bp polymerase chain reaction (PCR) products for SSCP analysis. (See Fig 3 legend for sequences of primers.) Primers were synthesized by the Protein Chemistry Core Facility at Washington University School of Medicine. The PCR for SSCP was performed using 200 ng genomic DNA in a total volume of 100  $\mu$ L (100 pmol of each primer, 200  $\mu$ mol/L of each dNTP, 1  $\mu$ L [10  $\mu$ Ci] per reaction of  $\gamma$ -<sup>32</sup>P[dCTP] [Amersham, Arlington Heights, IL], 2 mmol/L MgCl<sub>2</sub>, 1 $\times$  PCR buffer provided with the PCR kit [Perkin-Elmer, Norwalk, CT], and 2.5 U *Taq* DNA polymerase [Perkin Elmer]). A similar PCR was performed in the absence of  $\gamma$ -<sup>32</sup>P[dCTP], and the size of the PCR product was checked in 1% agarose gel. Thermal cycling (CoyTemp. Cycloer, Ann Arbor, MI) conditions were as follows. Initial denaturation of genomic DNA was set at 95°C for 5 minutes, followed by 30 cycles of denaturation at 94°C for 1 minute, annealing at 50°C for 1 minute, and extension at 72°C for 2 minutes. Ten microliters of the radiolabeled PCR products and 10  $\mu$ L loading buffer (95% formamide, 20 mmol/L EDTA, 0.05% bromophenol blue, and 0.05% xylene cyanol) were heated for 10 minutes at 95°C. Aliquots of 3  $\mu$ L were then loaded into each well of a 6% nondenaturing sequencing gel (acrylamide:bisacrylamide 100:1.5) containing 10% glycerol. In a parallel lane, nondenatured radiolabeled PCR products were also loaded. The nondenaturing gel was run in a cold room at 4°C to 6°C at 30 W for 5 hours. The gel was dried under vacuum at 80°C and exposed to x-ray film.

#### PCR and DNA Sequencing

The apo B gene region spanning nucleotides 6076 to 6470 was amplified using a PCR kit (Perkin Elmer). The forward primer started at nucleotide 6076 (5' CTC AAG ACC CAA TTT AAC 3'), and the reverse primer was complementary to the sequence 5' GGC TGC TCT GTA TTT TCT TAC 3'. The 394-bp PCR product was purified using a commercial kit (Promega, Madison, WI) and subcloned into the pGEMT vector (Promega). *Escherichia coli* JM109 was transformed with the recombinant plasmid by standard methods.<sup>21</sup> Plasmid DNA was prepared using a commercial kit (Wizard mini-prep, Promega), and 4  $\mu$ g plasmid DNA was used for the dideoxynucleotide sequencing.<sup>22</sup>

#### Allele-Specific Oligonucleotide Analysis

The allele-specific oligonucleotides (ASOS) had the following sequences: wild type 5' TACTGGACGAACTCTGGCTGAC 3'; and apo B-43.7 mutant, 5' TACTGGATGAACTCTGGCTGAC 3'. Oligonucleotides were 5' end labeled using  $\gamma$ -<sup>32</sup>P[ATP] (Amersham, Arlington Heights, IL). The total reaction volume of 20  $\mu$ L contained 10 pmol primers, 2  $\mu$ L 10 $\times$  kinase buffer, 5  $\mu$ L (50  $\mu$ Ci)  $\gamma$ -<sup>32</sup>P[ATP], and 1 U T4 DNA kinase (Boehringer Mannheim Biochemicals, Indianapolis, IN). The reaction was performed for

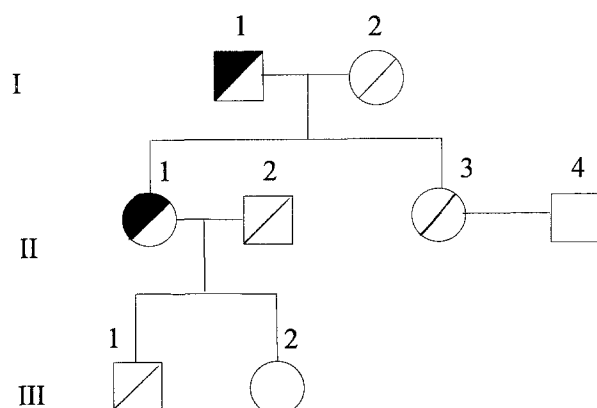


**Fig 1. Pedigree of the apo B-43.7 kindred. Apo B phenotypes and genotypes determined by Western blotting and SSCP are as follows: apo B-100/apo B-100 and apo B-100/apo B-43.7. II-1, the proband. Cross lines indicate that the subject has been tested. (□) Males; (○) females. Half-filled symbols indicate the presence of the apo B-43.7 truncated protein.**

30 minutes at 37°C and stopped by heating at 70°C for 5 minutes, and the radioactive products were purified with a Sephadex G-25 spin column (Boehringer Mannheim Biochemicals). Fifty microliters of the 394-bp PCR products (see above) were denatured with 0.2 mol/L NaOH at 95°C for 5 minutes, followed by addition of 800  $\mu$ L cold 15 $\times$  SSC (1 $\times$  SSC is 0.15 mol/L NaCl plus 0.015 mol/L sodium citrate). Samples were applied in duplicate to a nitrocellulose membrane (Schleicher and Schuell, Keene, NH) using a slot-blot apparatus. The membrane was baked at 80°C for 2 hours under vacuum and cut into two strips each containing an identical set of samples. Each strip was placed in a separate bag and prehybridized for 6 hours at 42°C in a solution containing 6 $\times$  SSC, 0.1% sodium dodecyl sulfate (SDS), and 10 $\times$  Denhardt solution,<sup>22</sup> followed by hybridization with radiolabeled wild-type ASO in one bag and mutant ASO in the other for 16 hours at 42°C. Washes were as follows: 6 $\times$  SSC for 5 minutes at room temperature, 2 $\times$  SSC/0.1% SDS for 30 minutes at room temperature, and 0.5 $\times$  SSC/0.1% SDS at 44°C for 30 minutes. Membranes were dried and exposed to x-ray film for 2 hours.

### The Metabolic Study

Detailed procedures for our metabolic protocols have been reported previously.<sup>23</sup> Briefly, the proband was requested not to change her diet 10 days before the study. Before the study began, the subject fasted for 10 hours to clear the plasma of any chylomicrons or remnants. Then a primed constant infusion of [ $1\text{-}^{13}\text{C}$ ]leucine (isotopic purity, 99%; MSD Isotopes, Montreal, Quebec, Canada) was started at 0.85 mg  $\cdot$  kg<sup>-1</sup> and immediately followed by an 8-hour constant infusion of the tracer at 0.85 mg  $\cdot$  kg<sup>-1</sup>  $\cdot$  h<sup>-1</sup>. After the infusion, the subject remained fasting for another 16 hours, noncaloric liquids were permitted. The subject then resumed her regular diet. A total of 32 plasma samples were drawn for determination of labeled plasma leucine enrichment. Of these, 21 were used to assay apo B leucine enrichment. Blood was collected into EDTA-containing tubes, and the plasma was separated by low-speed centrifugation. VLDL (d 1.006 g  $\cdot$  mL<sup>-1</sup>), IDL (d 1.006 to 1.019 g  $\cdot$  mL<sup>-1</sup>), LDL (d 1.019 to 1.063 g  $\cdot$  mL<sup>-1</sup>), and HDL (d 1.063 to 1.2 g  $\cdot$  mL<sup>-1</sup>) were isolated by sequential ultracentrifugation and dialyzed against ammonium bicarbonate (5 mmol/L) for 24 hours. Apo B concentrations were measured in VLDL, IDL, LDL, and HDL fractions by enzyme-linked immunosorbent assay and confirmed by protein assays<sup>24</sup> as previously described.<sup>23</sup> Apo B-100 and Apo B-43.7 in the lipoprotein fractions were then separated by SDS-polyacrylamide gel electrophoresis (PAGE) and stained with Coomassie blue.<sup>25</sup> Protein bands corresponding to apo B-100 were scanned by laser densitometry. Pool sizes for apo B-100 were estimated by scanning five samples from different time points in each lipoprotein subfraction and averaging the ratios. Total apo B-100 was the proportion of apo B-100 times total apo B; total apo B-43.7 was the difference. VLDL, IDL, and LDL apo B-100 pool sizes were determined by multiplying the measured apo B concentrations by the proportion of total apo B concentrations represented by apo B-100 and by plasma volume (body weight  $\times$  0.045). VLDL and HDL apo B-43.7 pools were determined by multiplying total apo B-43.7 by the proportion of apo B-43.7 in the two fractions as determined by DGUC followed by immunoblotting of density fractions.

### Isolation of Apo B and Plasma Amino Acids

Plasma amino acids were isolated by cation-exchange chromatography.<sup>26</sup> Apo B-100 and apo B-43.7 bands isolated by SDS-PAGE (3% to 6%) were excised, hydrolyzed in 12N HCl for 16 hours at 100°C, and derivatized to *n*-acetyl-*n*-propanol esters.<sup>27</sup> Enrich-

ments were determined by gas chromatography-mass spectrometry<sup>27</sup> and subsequently converted to tracer to tracee ratios.<sup>28</sup>

### Kinetic Analysis

The CONSAM program<sup>29</sup> was used to fit the model to the observed kinetic tracer data and lipoprotein subfraction relative mass distributions for both apo B-100 and apo B-43.7. A forcing function was used to describe the plasma leucine tracer to tracee ratio during and after termination of the 8-hour primed continuous tracer infusion period.

The compartmental model used for the VLDL, IDL, and LDL apo B-100 subsystem was a minor modification of the model previously described.<sup>23</sup> Although the numbering of the compartments may be arbitrary, compartment numbers used for the apo B-100 system correspond to those used previously.<sup>23</sup> The model consists of a plasma amino acid compartment (compartment 1) and an intracellular compartment with a rapid turnover rate accounting for isotopic dilution of tracer amino acid (compartment 9). Compartments 10 and 11 account for the plasma kinetics of VLDL apo B-100 and represent a minimal delipidation chain. VLDL apo B-100 with a fast rate of turnover (compartment 10) can leave the plasma or be converted to slow VLDL (compartment 11). IDL apo B-100 (compartment 20) arises from both fast and slow VLDL. LDL apo B-100 (compartment 30) is derived from the IDL fraction or directly from fast VLDL. The fractional catabolic rate (FCR) of a given compartment is the sum of individual rate constants leaving that compartment; the FCR of VLDL apo B-100 is the weighted average (related to mass distribution) of the FCR of compartments 10 and 11. Since all apo B-100 enters plasma as fast VLDL, apo B-100 secretion rate was determined as the size of compartment 10 [(total VLDL apo B-100 pool size)  $\times$  (model-derived percent of VLDL apo B-100 in compartment 10)] times the FCR of compartment 10.

A compartmental model of the apo B-43.7 subsystem was developed independently of the apo B-100 subsystem. The comparison against the apo B-100 subsystem allows the latter to serve as an internal control representing the metabolism of "normal" apo B-containing particles.

## RESULTS

### The Kindred and the Truncation

The proband (II-1) manifested low cholesterol and low apo B levels and also an apo B truncation that had an apparent molecular weight between that of apo B-42 and apo B-45 (Fig 2). Her father (I-1) had approximately 25th-percentile TC levels, less than 10th-percentile LDL cholesterol, and less than 10th-percentile apo B. He also had an apo B-43.7 band. Although two other members also had approximately 25th-percentile cholesterol and less than average apo B levels, they had no detectable truncations.

### The Molecular Genetic Defect

Since the SDS gel yielded molecular weights between those of apo B-42 and apo B-45 on different analyses, by using SSCP we restricted the stretch of DNA that needed to be sequenced. The site of the mutation appeared to reside in a 217-base DNA segment in exon 26 (positions 6076 to 6293; Fig 3). After subcloning and sequencing the fragment, the mutation consisted of a C  $\rightarrow$  T change at position 6162, converting the arginine codon CGA to a stop codon TGA

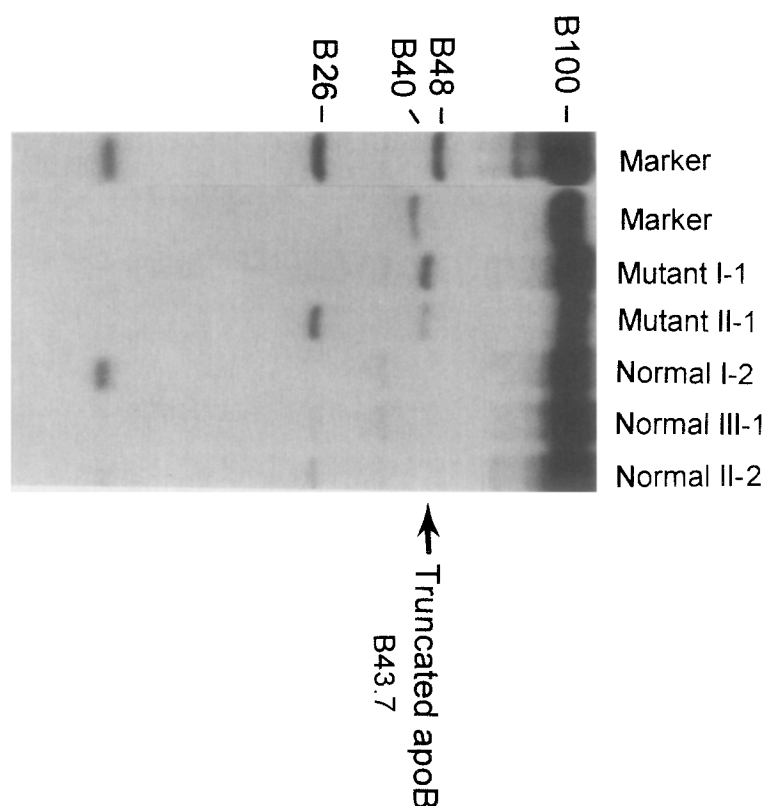


**Fig 2.** Identification of the truncated apo B species by Western blotting analysis. Lanes are labeled to correspond with the pedigree positions in Fig 1. Marker, contains apo B from a subject with hypertriglyceridemia and a normal subject. Positions of apo B-100, B-48, B-40, and B-26 are marked; the lowest band is unidentified.

(data not shown). Seven of 15 clones analyzed had the C → T change and the rest contained a T, confirming the heterozygosity of the proband. The predicted protein contains 1,985 amino acid residues, and is designated as apo B-43.7 (number of amino acids in truncation/number of amino acids in apo B-100 =  $1,985/4,536 \times 100$ ).

On ASO analysis, subjects I-1 and II-1, who expressed the FHBL phenotype and the truncated form of apo B-43.7,

also had the mutant allele, but other members of the kindred did not (Fig 4).

#### *Distribution of Apo B-100 and Apo B-43.7 Among the Major Size and Density Classes of Lipoproteins*

On FPLC (Fig 5), greater than 90% of apo B-43.7 was detected in particles that eluted with LDL and between LDL and HDL (peak fraction no., 34 for subject I-1 [A] and

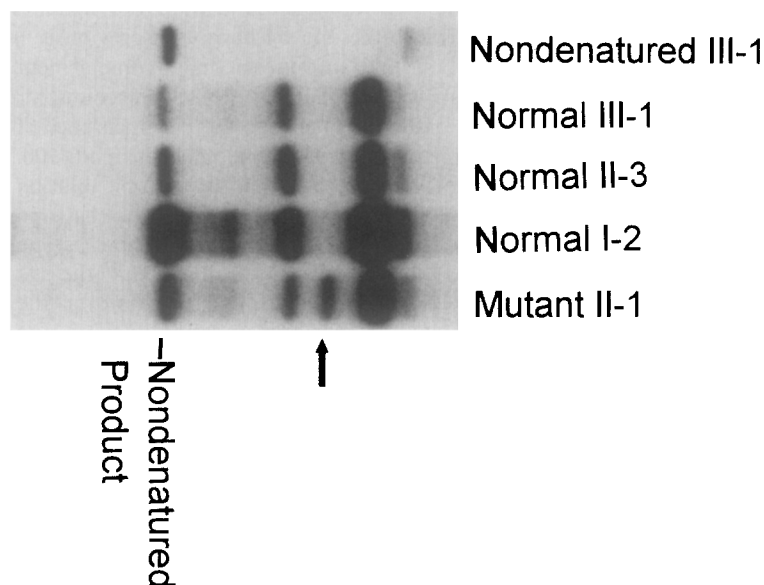


**Fig 3.** SSCP. To identify the region of the apo B gene containing the mutation leading to a truncated apo B, PCR was performed in the presence of [ $\gamma$ - $^{32}$ P]dCTP. The forward primer started at position 6076 (5' CTC AAG ACC CAA TTT AAC 3'); the reverse primer complementary to sequence 5' AAC AAT TGT AAA TTC TTG GGG 3' ended at nucleotide 6293. The PCR product consisting of 210 bp was identified on 1% agarose gel electrophoresis. An aliquot of the PCR product of each member of the kindred was denatured and separated in a 6% nondenaturing gel containing 10% glycerol. Lanes are marked as in Fig 1. Arrow, the novel band due to the mutation.

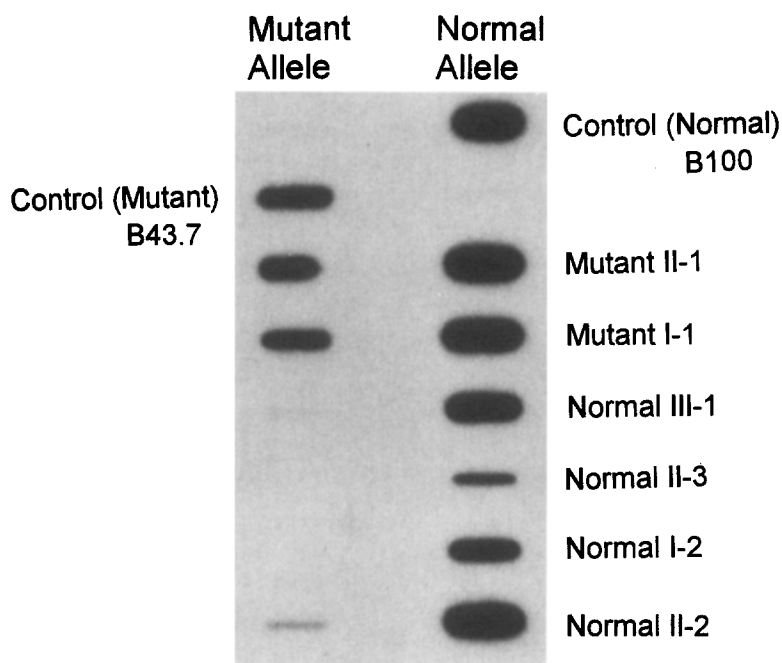


Fig 4. ASO analysis. ASO was performed further to confirm the apo B-43.7 mutation and to identify other affected members in the kindred. The region of the genomic DNA containing the mutation was amplified by PCR as in Fig 3. PCR products were applied to the nitrocellulose membrane in 2 parallel lanes using a slot-blot apparatus. The lanes were cut apart, and half of the membrane was probed with the wild-type (apo B-100) and the other with the mutant (apo B-43.7)  $^{32}\text{P}$  end-labeled ASO. Recombinant plasmids containing the mutant or wild-type alleles were used as positive controls. Faint bands to the left of normals II-2 and III-1 represent nonspecific annealing of a slight amount of labeled mutant ASO.

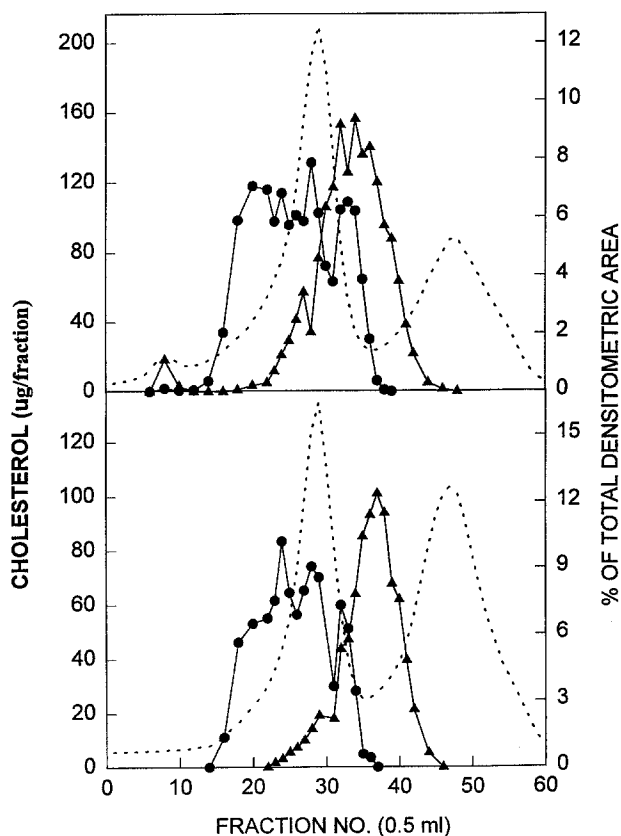


Fig 5. Gel permeation chromatographic profiles of apo B-100- and apo B-43.7-containing lipoproteins. Subjects no. I-1 and II-1 are shown in A and B, respectively. (.....) Cholesterol ( $\mu\text{g}/\text{fraction}$ ); (●) apo B-100; (▲) apo B-43.7 (% of total). Normal VLDL, IDL, LDL, and HDL elute in fractions 1 to 10, 11 to 22, 23 to 35, and 36 to 60, respectively.

37 for subject II-1 [B]). Approximately 5% of apo B-43.7 eluted with IDL-sized particles. On DGUC (Fig 6 and Table 2), approximately 60% of apo B-43.7 floated with particles denser than LDL in subject I-1 (peak fraction no., 28; Fig 6A), and about 60% floated at the density of HDL in subject II-2 (peak fraction no., 40; Fig 6B). Thirty percent to 40% of apo B-43.7 floated at VLDL-IDL densities in both subjects (fractions no. 1 to 6).

#### Metabolism of Apo B-100 and Apo B-43.7

The compartmental model for apo B-100 and apo B-43.7 (Fig 7) represents the minimal structural complexity necessary and sufficient to account for both the observed isotopic enrichment data and apo B relative mass distribution between lipoprotein subfractions. The apo B-100 model is essentially identical to the one we have used previously,<sup>23</sup> with the exception that an intermediate compartment (compartment 9) was included to explicitly account for isotopic dilution and delays between the disappearance of tracer leucine from plasma and its emergence in apo B-100. Furthermore, the explicit inclusion of this isotopic dilution compartment allowed us to test the hypothesis that apo B-43.7 was derived from the same precursor pool as apo B-100. Many apo B-100 models more complex than the one used herein may be found in the literature; however, the present data collected from a primed continuous infusion protocol lack sufficient information to resolve any structural complexity above that which is shown.

The model for the apo B-100 subsystem suggests that there was no direct removal of slow VLDL (compartment 11) or IDL (compartment 20) particles from plasma, but there was complete conversion of slow VLDL to IDL and LDL particles (Figs 7A and 8B). Minor variations of this model that allowed for direct-loss pathways from these compartments without conversion to more dense subfrac-

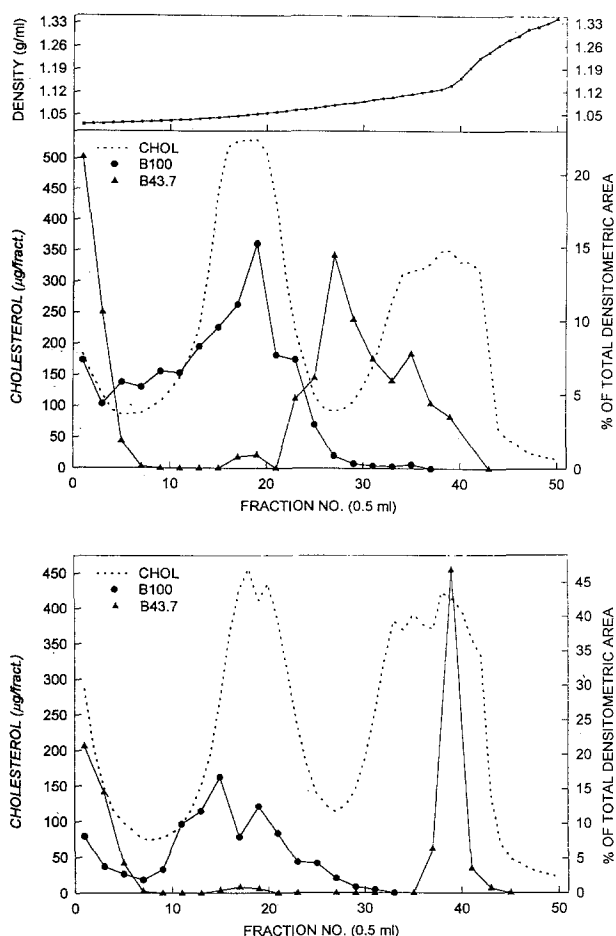


**Fig 6.** DGUC profiles of apo B-100- and apo B-43.7-containing lipoproteins. Subjects no. I-1 and II-1 are shown in A and B, respectively. (.....) Cholesterol ( $\mu\text{g}/\text{fraction}$ ); (●) apo B-100; (▲) apo B-43.7 (% of total). Normal VLDL and IDL float in fractions 1 to 10, LDL in fractions 11 to 25, and HDL in fractions 26 to 45.

tions were evaluated and rejected because they did not improve the fit to the kinetic data and adversely affected the relative mass of the apo B-100 subfraction. The model-derived relative mass distributions were in close agreement with the observed distribution of 15.6%, 1.5%, and 82.9% in VLDL, IDL, and LDL, respectively (Fig 6 and Table 2). At plateau, plasma VLDL apo B-100 achieved 83% of the enrichment of plasma leucine, ie, the plasma accounted for 83% of the flux of leucine into apo B-100; the remaining 17% was derived from an unlabeled leucine pool. Plasma concentrations for apo B-100 and apo B-43.7 and production rates and FCRs for apo B-100 lipoprotein are shown in Table 2.

The model developed for the apo B-43.7 subsystem (Fig 7B) was the simplest that was consistent with both the kinetic tracer data (Fig 8C) and the observed apo B-43.7 subfraction relative mass distribution (40% and 60% in VLDL and HDL, respectively; Fig 6 and Table 2). It was necessary to postulate that the isotopic dilution of the precursor pool for apo B-43.7 was considerably greater than for apo B-100 such that the two proteins could not share a common precursor amino acid pool. An additional delay

(0.55 hours) was necessary to account for the appearance of tracer in VLDL apo B-43.7; however, there was no delay apparent for the appearance of tracer in HDL apo B-43.7. The model postulates that the protein observed in the HDL subfraction is derived from both direct synthesis and conversion from VLDL (Fig 7B). Several variations of this model were tested and rejected. For example, omission of the direct HDL synthesis pathway resulted in tracer peaking in HDL later than was observed, and the projected relative mass distribution of protein between VLDL and HDL (28% and 72% in VLDL and HDL, respectively) was not equal to that observed. In a second variation, omission of the VLDL to HDL conversion pathway resulted in tracer peaking earlier in HDL than was observed, although a good agreement with the observed mass distribution was achieved. In a third variation, complete conversion of VLDL to HDL without any direct loss of VLDL resulted in a reasonable fit to the VLDL and HDL kinetic tracer data, but the relative mass distribution (13% and 87% in VLDL and HDL, respectively) was inconsistent with the observed distribution. Inclusion of all pathways illustrated in Fig 7B was necessary and sufficient to fit both the observed kinetic tracer data and the relative apo B-43.7 mass distribution (Table 2).

The total production rate of apo B-43.7 was 31% of that

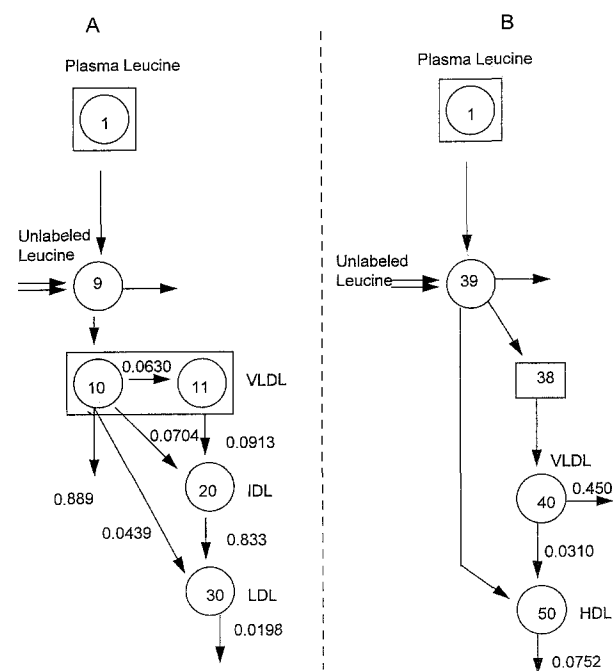


**Fig 7.** Multicompartmental model for apo B-100. (A) Model for apo B-100; (B) model for apo B-43.7. Compartment 1, plasma leucine tracer to tracee ratio; compartment 9, input of unlabeled leucine for assembly of apo B-100-containing lipoproteins; compartments 10 and 11, fast and slow VLDL apo B-100, respectively; compartment 20, IDL apo B-100; compartment 30, LDL apo B-100; compartment 38, delay compartment for apo B-43.7; compartment 39, input of unlabeled leucine for assembly of apo B-43.7-containing lipoproteins; compartment 40, VLDL apo B-43.7; compartment 50, HDL apo B-43.7. Metabolic pathways are labeled with fractional rate constants (pools/h) for conversion of 1 compartment to another.

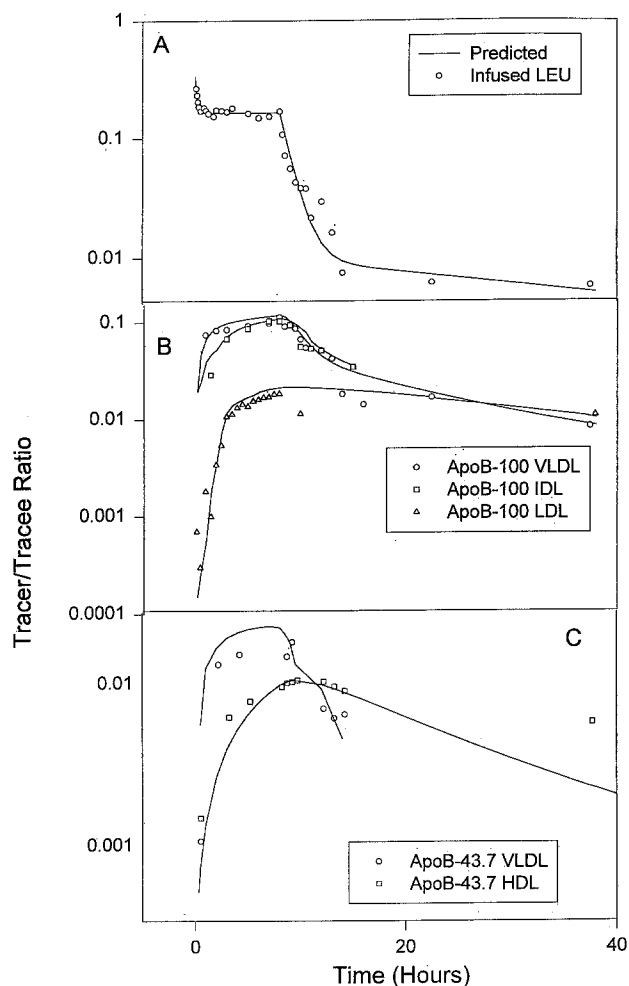


**Fig 8.** Incorporation of infused  $^{13}\text{C}$ -leucine into plasma leucine and plasma lipoproteins. Data are from subject no. II-1. (A) Tracer to tracee ratios in plasma leucine; (B) incorporation of  $^{13}\text{C}$ -leucine into VLDL apo B-100, IDL apo B-100, and LDL apo B-100; (C) incorporation of  $^{13}\text{C}$ -leucine into VLDL apo B-43.7 and HDL apo B-43.7. Symbols are observed values; lines are drawn by multicompartmental model analysis.

of apo B-100 ( $9.6 \pm 31.3 \text{ mg} \cdot \text{kg}^{-1} \cdot \text{d}^{-1}$ ), ie, less than the 43.7% that would be expected on a molar basis (Table 2). Eighty-six percent of the production appeared in VLDL and 14% in HDL. Of the apo B-43.7 that appeared in HDL, 70% was derived from direct synthesis (compartment 39) and 30% from VLDL (compartment 40). The model projects that enrichment of apo B-43.7 would be only 14% of plasma leucine enrichment. FCRs of the two VLDL populations were similar. The FCR of apo B-43.7 HDL was higher than that of apo B-100 LDL (Table 2).

#### DISCUSSION

We present a newly discovered apo B truncation, apo B-43.7, in two generations of a kindred with FHBL. We present the genetic defect, distribution of the truncation among plasma lipoproteins, and its metabolism. In the apo B-43.7/apo B-100 heterozygote proband, TC, LDL choles-

terol, and apo B levels were very low (<5th percentile; Table 1). The low LDL cholesterol/low apo B phenotype cosegregated with the apo B-43.7 mutation in the kindred (Fig 1). The father's LDL cholesterol and apo B levels were at the 10th percentile for his age, gender, and race, and he also had the truncation and gene defect. There may be more than one cause for low cholesterol in this kindred, since the mother of the proband has less than 25th-percentile LDL cholesterol totals (no truncation). Thus, less than average LDL cholesterol levels are common in the kindred, but the lowest-percentile levels tend to be associated with the apo B-43.7 truncation.

Sufficient ambiguity for the molecular weight of the truncated apo B remained on SDS-PAGE to require the use of SSCP (Fig 3) to narrow the region of DNA to be sequenced. The mutation was shown to be a nonsense mutation consisting of a base conversion ( $\text{C} \rightarrow \text{T}$ ), changing an Arg codon to a termination signal (Fig 4). A  $\text{C} \rightarrow \text{T}$  change occurs frequently.<sup>1,5</sup> The mutation was confirmed by ASO analysis (Fig 4).

Only about 5% of apo B-43.7 was present in the IDL size range on FPLC, but 30% to 40% was present at VLDL-IDL density on DGUC, suggesting that the apo B-43.7 truncation-containing LDL- and IDL-size particles could float as VLDL/IDL-density particles. Apo B-43.7 VLDL/IDL-density particles could be derived from the liver and intestine, but we found no apo B-48 in plasma samples taken after 12 hours of fasting, suggesting that in the fasted state most apo B-43.7 may have been derived from the liver.<sup>30</sup> Young et al<sup>10</sup> and Groenewegen et al<sup>7</sup> also have reported the presence of some short apo B truncations in the VLDL-density range.

It is likely that the mutant VLDL/IDL-density particles are metabolically analogous to apo B-100-containing VLDL. But instead of being converted to LDL-density particles, mutant particles seem to be converted to HDL-density particles (Figs 7 and 8). Longer truncations, eg, apo B-89- and apo B-75-containing VLDLs (isolated by ultracentrifugation) are converted from VLDLs to IDLs and LDLs that are smaller than normal, similar to their apo B-100-

**Table 2.** Metabolic Kinetic Parameters for Apo B-100 and Apo B-43.7

Parameter	Apo B-100	Apo B-43.7
FCR (pools $\cdot \text{d}^{-1}$ )		
VLDL	16.03	11.78
IDL	19.99	NA
LDL	0.456	NA
HDL	NA	1.8
Production rate ( $\text{mg} \cdot \text{kg}^{-1} \cdot \text{d}^{-1}$ )	31.3	9.6
Relative mass distribution (%)		
VLDL	15.6 (13)	42.2 (40)
IDL	1.5 (5)	NA
LDL	82.9 (82)	NA
HDL	NA	57.8 (60)
Plasma concentration (mg/dL)	36	4

NOTE. Values in parentheses are based on DGUC.

Abbreviation: NA, not applicable, ie, protein not found in this subfraction.

containing counterparts.<sup>16,23</sup> It is likely that lipoprotein lipase catalyzed the remodeling of apo B truncation-containing lipoproteins, since lipoprotein lipase interacts with apo B-containing lipoproteins at the NH<sub>2</sub>-terminal region of apo B,<sup>31</sup> which all COOH-terminal truncations possess.

The finding that 83% of the leucine incorporated into VLDL apo B-100 was derived from plasma leucine is in good agreement with an earlier study in which leucine enrichment in VLDL apo B-100 was 94% of the enrichment of plasma leucine,<sup>32</sup> and is consistent with similar percentages in previous studies from this laboratory.<sup>16,23</sup> However, the larger tracer dilution for leucine incorporated into apo B-43.7 predicted by the model (14% of leucine derived from plasma and 86% from other unlabeled sources) strongly suggests that apo B-43.7 and apo B-100 were derived from different intracellular pools. We also observed that apo B-89<sup>23</sup> and apo B-75<sup>16</sup> achieved essentially the same isotopic enrichment as apo B-100, consistent with the hypothesis that these two truncations were derived from the same intrahepatic precursor pools as their apo B-100 counterparts. However, apo B-31 was considerably less enriched than apo B-100 at plateau enrichment.<sup>33</sup> The finding that the precursor pool for short truncations of apo

B undergoes a greater isotopic dilution than the hepatic apo B-100 precursor pool suggests production of these truncations by other tissues. As noted, the intestine could be another tissue site of production in the case of apo B-31 and apo B-43.7.<sup>30</sup>

We observed that the apo B-43.7 secretion rate was 31% of that for apo B-100 within the same subject. This is in agreement with our previous studies<sup>16,23</sup> showing that the truncated apo B secretion rate relative to apo B-100 within the same subject decreases as the size of apo B decreases. However, in contrast with previous results<sup>33,34</sup> in which apo B-100 production rates were lower than normal, in this case apo B-100 production was similar to normal levels.

In summary, we have demonstrated that mutations as short as apo B-43.7 may be secreted into plasma VLDL/IDL-density particles and may be converted to HDL-density particles, thus mimicking the apo B-100 metabolic pathway.

#### ACKNOWLEDGMENT

The authors thank Tom Kitchens for expert technical assistance. We also express our gratitude to Mary Lou Rheinheimer for preparation of the manuscript.

#### REFERENCES

1. Linton MF, Farese RV Jr, Young SG: Familial hypobetalipoproteinemia. *J Lipid Res* 34:521-541, 1993
2. Kane JP: Apolipoprotein B: Structural and metabolic heterogeneity. *Annu Rev Physiol* 45:637-650, 1983
3. Powell LM, Wallis SC, Pease RJ, et al: A novel form of tissue-specific RNA processing produces apolipoprotein B-48 in intestine. *Cell* 50:831-840, 1987
4. Goldstein JL, Brown MS: The low density lipoprotein pathway and its relation to atherosclerosis. *Annu Rev Biochem* 46:897-930, 1977
5. Groenewegen WA, Krul ES, Schonfeld G: The apolipoprotein B-52 mutation associated with hypobetalipoproteinemia is compatible with a misaligned pairing deletion mechanism. *J Lipid Res* 34:971-981, 1993
6. Talmud PJ, Krul ES, Pessah M, et al: Donor splice mutation generates a lipid-associated apolipoprotein B-27.6, in a patient with homozygous hypobetalipoproteinemia. *J Lipid Res* 35:468-477, 1994
7. Groenewegen WA, Aversa M, Krul ES, et al: Apolipoprotein B-38.9 does not associate with apo(a) and forms two distinct HDL density particle populations that are larger than HDL. *J Lipid Res* 35:1012-1025, 1994
8. Groenewegen WA, Krul ES, Aversa MR, et al: Dysbetalipoproteinemia in a kindred with hypobetalipoproteinemia due to mutations in the genes for apo B (apo B-70.5) and apo E (apo E2). *Arterioscler Thromb* 14:1695-1704, 1994
9. Young SG, Hubl ST, Smith RS, et al: Familial hypobetalipoproteinemia caused by a mutation in the apolipoprotein B gene that results in a truncated species of apolipoprotein B (B-31). A unique mutation that helps to define the portion of the apolipoprotein B molecule required for the formation of buoyant, triglyceride-rich lipoproteins. *J Clin Invest* 85:933-942, 1990
10. Young SG, Hubl ST, Chappell DA, et al: Familial hypobetalipoproteinemia associated with a mutant species of apolipoprotein B (B-46). *N Engl J Med* 320:1604-1610, 1989
11. Krul ES, Kinoshita M, Talmud P, et al: Two distinct truncated apolipoprotein B species in a kindred with hypobetalipoproteinemia. *Arteriosclerosis* 9:856-868, 1989
12. Wagner RD, Krul ES, Tang J, et al: Apo B-54.8, a truncated apolipoprotein found primarily in VLDL, is associated with non-sense mutation in the apo B gene and hypobetalipoproteinemia. *J Lipid Res* 32:1001-1011, 1991
13. Fazio S, Sidoli A, Vivenzio A, et al: A form of familial hypobetalipoproteinemia not due to a mutation in the apolipoprotein B gene. *J Intern Med* 229:41-47, 1991
14. Hardman DA, Pullinger CR, Hamilton RL, et al: Molecular and metabolic basis for the metabolic disorder normotriglyceridemic abetalipoproteinemia. *J Clin Invest* 88:1722-1729, 1991
15. Lipid Research Clinics Program: Manual of Laboratory Operations, vol 1: Lipid and Lipoprotein Analysis. DHEW Publication No. (NIH) 75:628. Washington, DC, US Government Printing Office, 1974
16. Krul ES, Parhofer KG, Barrett PHR, et al: Apo B-75, a truncation of apolipoprotein B associated with familial hypobetalipoproteinemia: Genetic and kinetic studies. *J Lipid Res* 33:1037-1050, 1992
17. Srivastava RAK, Tang J, Krul ES, et al: Dietary fatty acids and dietary cholesterol differ in their effect on the in vivo regulation of apolipoprotein AI and AII gene expression in inbred strains of mice. *Biochim Biophys Acta* 1125:251-261, 1992
18. Krul ES, Kleinman Y, Kinoshita M, et al: Regional specificities of monoclonal anti-human apolipoprotein B antibodies. *J Lipid Res* 29:937-948, 1988
19. Orita M, Iwahana H, Kanazawa H, et al: Detection of polymorphism of human DNA by gel electrophoresis as single-strand conformation polymorphisms. *Proc Natl Acad Sci USA* 86:2766-2770, 1989
20. Orita M, Suzuki Y, Sekiya T, et al: Rapid and sensitive detection of point mutation and DNA polymorphism using the polymerase chain reaction. *Genomics* 5:874-879, 1989



21. Maniatis T, Fritsch ER, Sambrook J: *Molecular Cloning: A Laboratory Manual*. Cold Spring Harbor, NY, Cold Spring Harbor Laboratory, 1982
22. Mierendorff RC, Pfeffer DC: Direct sequencing of denatured plasmid DNA. *Methods Enzymol* 152:556-562, 1987
23. Parhofer KG, Barrett PH, Bier D, et al: Lipoproteins containing the truncated apolipoprotein, apo B-89, are cleared from human plasma more rapidly than apo B-100 containing lipoproteins in vivo. *J Clin Invest* 89:1931-1937, 1992
24. Lowry OH, Rosebrough NJ, Farr AL, et al: Protein measurement with the Folin phenol reagent. *J Biol Chem* 193:265-275, 1951
25. Laemmli UK: Cleavage of structural proteins during the assembly of the head of bacteriophage T4. *Nature* 227:680-685, 1970
26. Adams RF: Determination of amino acid profiles in biological samples by gas chromatography. *J Chromatogr* 95:189-212, 1974
27. Matthews DE, Ben-Galim E, Bier DM: Determination of stable isotopic enrichment in individual plasma amino acids by chemical ionization mass spectrometry. *Anal Chem* 51:80-84, 1979
28. Cobelli C, Toffolo G, Foster DM: Tracer-to-tracee ratio for analysis of stable isotope tracer data: Link with radioactive kinetic formalism. *Am J Physiol* 262:E968-E975, 1992
29. Boston RC, Greif PC, Berman M: Conversational SAAM—An interactive program for kinetic analysis of biological systems. *Comput Biomed Res* 13:111-119, 1981
30. Krul ES, Tang J, Kettler TS, et al: Lengths of truncated forms of apolipoprotein B (APOB) determine their intestinal productions. *Biochem Biophys Res Commun* 189:1069-1076, 1992
31. Choi SY, Sivaram P, Walker DE, et al: Lipoprotein lipase association with lipoproteins involves protein-protein interactions with apolipoprotein B. *J Biol Chem* 270:8081-8086, 1995
32. Reed PJ, Hachey DL, Patterson BW, et al: VLDL apolipoprotein B-100, a potential indicator of the isotopic labeling of the hepatic protein synthetic precursor pool in humans: Studies with multiple stable isotopically labeled amino acids. *J Nutr* 122:457-466, 1992
33. Parhofer KG, Barrett PHR, Aguilar-Salinas CA, et al: Positive linear correlation between the length of truncated apolipoprotein B and its secretion rate (in vivo studies in apo B-89, apo B-75, apo B-54.8 and apo B-31 heterozygotes). *J Lipid Res* 37:844-852, 1996
34. Aguilar-Salinas CA, Carlos A, Barrett PHR, et al: Apoprotein B-100 production is decreased in subjects heterozygous for truncations of apoprotein B. *Arterioscler Thromb Vasc Biol* 15:71-80, 1995